

**A COMPARISON OF MARCHING-ON IN TIME
METHOD WITH MARCHING-ON IN DEGREE
METHOD FOR THE TDIE SOLVER**

B. H. Jung

Department of Information and Communication Engineering
Hoseo University
Asan, Chungnam 336-795, Korea

Z. Ji

Laird Technologies
3425 N. 44th St. Lincoln, NE 68504, USA

T. K. Sarkar

Department of Electrical Engineering and Computer Science
Syracuse University
Syracuse, NY 13244-1240, USA

M. Salazar-Palma

Dpto. SSR, E.T.S.I. Telecomunicacion
Universidad Politecnica de Madrid
Ciudad Universitaria s/n, 28040 Madrid, Spain

M. Yuan

Cadence Design Systems Inc.
1620 W. Fountainhead Pkwy, Suite 219, Tempe, AZ 85282, USA

Abstract—One of the most popular methods to solve a time-domain integral equation (TDIE) is the marching-on in time (MOT) method. Recently, a new method called marching-on in degree (MOD) that uses Laguerre polynomials as temporal basis functions has been developed to eliminate the late time instability of the MOT method. The use of an entire domain basis for the time variable eliminates the requirement of a Courant condition, as there is no time variable involved in the field calculation. This is possible as in the procedure the time and the space variables can be separated analytically. A comparison is presented

between these two methods from the standpoint of formulation, stability, cost, and accuracy. Numerical results are presented to illustrate these features in the comparison.

1. INTRODUCTION

The electromagnetic community has been seriously engaged in the numerical solution of TDIE for over twenty years [1–15]. An integral equation method requires only a surface discretization that is sometimes preferred over the differential one using a volumetric discretization and does not need absorbing boundary conditions [16–18]. Furthermore TDIE implicitly impose the radiation condition and there exists no grid dispersion. As a time-domain technique, it analyzes wide-band and potentially time-varying and nonlinear phenomena in one single analysis.

The most popular method to solve a TDIE is the time-marching scheme. However, as pointed out by many researchers, the time-marching method may suffer from its late-time instability. Much work has been done to eliminate the instability [5–15]. In some studies [5, 13], it has been shown that the instabilities arising in MOT solvers are due to low- and high-frequency modes that creep into the solution and that can be eliminated by a combination of spatial and temporal averaging. The disadvantage of these approaches is that they may lose some accuracy during the solution, and it is difficult to apply to complex objects. Other studies have indicated that the cause of instability is that if the temporal basis function has a rich high-frequency content, the spatial discretization may not be enough for these high frequencies. The accumulated error will lead to late-time instability. A proper choice of temporal basis functions can improve the stability [6–8].

In [6–8], the temporal basis functions are still piecewise functions and the temporal testing uses point matching method. Recently, Sarkar's group developed a new method called MOD method [19–23]. Instead of piecewise temporal basis function, a set of entire domain basis function which is called the weighted Laguerre polynomials have been used. There are four characteristic properties of the weighted Laguerre polynomials [24, 25] that have been used in this new formulation:

- 1) Causality: The Laguerre polynomials are defined for $0 \leq t < +\infty$. Therefore, they are quite suitable to represent any natural time-domain responses as they are always causal.

- 2) Recursive computation: The Laguerre polynomials of higher degrees can be generated recursively.
- 3) Orthogonality: With respect to a weighting function, the Laguerre polynomials are orthogonal with respect to each other. One can construct a set of orthogonal basis functions, which we call the weighted Laguerre polynomials. Physical quantities that are functions of time can be spanned in terms of these orthogonal basis functions—weighted Laguerre polynomials.
- 4) Stability: The weighted Laguerre polynomials decay to zero as time goes to infinity and therefore the solution do not blow up for late times. Also, because the weighted Laguerre polynomials form an orthonormal set, any arbitrary time function can be spanned by these basis functions.

When using the Galerkin's method the Laguerre polynomials are used as temporal basis for testing procedures, which is similar to the spatial testing procedure of the method of moments. By applying the temporal testing procedure to the TDIE, the numerical instabilities associated with the MOT procedure can be eliminated. Due to the property of the weighted Laguerre functions, the spatial and the temporal variables can be completely separated and the time variable can be completely eliminated from all the computations except the calculation of the excitation coefficient that is determined by the excitation waveform only. This eliminates the need of interpolation that is necessary to estimate values of the current or the charge at time instances that do not correspond to a sampled time instance. Therefore the values of the current can be obtained at any time exactly and no time step is needed as in the MOT method.

In this work, we present a comparison of these two numerical methods. The comparison is made through some numerical examples including stability, cost, and accuracy. It is hoped that this comparison might help in choosing one method over the other for a given situation.

This paper is organized as follows. In the next section, for the sake of completeness, we present a brief description of general TDIE, MOT and MOD algorithms. In Section 3, numerical results are presented to show the comparison between these two methods. Finally, in Section 4, we present the conclusions drawn from this study.

2. FORMULATION

2.1. TD-EFIE, TD-MFIE, and TD-CFIE

Let S represent the surface of a closed conducting body in free space illuminated by a transient electromagnetic wave with the electric field

$\mathbf{E}^i(\mathbf{r}, t)$ and magnetic field $\mathbf{H}^i(\mathbf{r}, t)$. The incident fields will induce a surface current $\mathbf{J}(\mathbf{r}, t)$ on S that radiates the scattered electric field $\mathbf{E}^s(\mathbf{r}, t)$ and magnetic field $\mathbf{H}^s(\mathbf{r}, t)$. From the boundary conditions, we obtain the time-domain electric field integral equation (TD-EFIE) and the time-domain magnetic field integral equation (TD-MFIE), respectively,

$$\left[\dot{\mathbf{E}}^i(\mathbf{r}, t) + \dot{\mathbf{E}}^s(\mathbf{r}, t) \right]_{\text{tan}} = 0 \quad (1)$$

$$\mathbf{n} \times [\dot{\mathbf{H}}^i(\mathbf{r}, t) + \dot{\mathbf{H}}^s(\mathbf{r}, t)]_{\text{tan}} = \dot{\mathbf{J}}(\mathbf{r}, t). \quad (2)$$

The subscript ‘tan’ denotes the tangential component. Here, the derivative is taken to avoid the computation of charge accumulation in TD-EFIE. The dot on the top of the variable represents a temporal derivative.

The scattered electric field $\mathbf{E}^s(\mathbf{r}, t)$ and magnetic field $\mathbf{H}^s(\mathbf{r}, t)$ can be expressed in terms of the vector potentials \mathbf{A} and scalar potentials Φ ,

$$\mathbf{E}^s(\mathbf{r}, t) = -\dot{\mathbf{A}}(\mathbf{r}, t) - \nabla\Phi(\mathbf{r}, t) \quad (3)$$

$$\mathbf{H}^s(\mathbf{r}, t) = \frac{1}{\mu_0} \nabla \times \mathbf{A}(\mathbf{r}, t) \quad (4)$$

where \mathbf{A} and Φ are given by the retarded integral equations involving the electric surface current density \mathbf{J} and the surface charge density q , respectively,

$$\mathbf{A}(\mathbf{r}, t) = \frac{\mu_0}{4\pi} \int_S \frac{\mathbf{J}(\mathbf{r}', \tau)}{R} dS \quad (5)$$

$$\Phi(\mathbf{r}, t) = \frac{1}{4\pi\epsilon_0} \int_S \frac{q(\mathbf{r}', \tau)}{R} dS \quad (6)$$

where R represents the distance between the observation point \mathbf{r} and the source point \mathbf{r}' , $\tau = t - R/c$ is the retarded time, μ_0 and ϵ_0 are permeability and permittivity of free space, and c is the velocity of propagation of the electromagnetic wave in free space. The charge density q is related to \mathbf{J} by the equation of continuity

$$\nabla \cdot \mathbf{J}(\mathbf{r}, t) = -\frac{\partial}{\partial t} q(\mathbf{r}, t). \quad (7)$$

Extracting the Cauchy principal value from the curl term in (4), the scattered magnetic fields $\dot{\mathbf{H}}^s(\mathbf{r}, t)$ can be written as

$$\mathbf{n} \times \dot{\mathbf{H}}^s(\mathbf{r}, t) = \frac{\dot{\mathbf{J}}(\mathbf{r}, t)}{2} + \mathbf{n} \times \frac{1}{4\pi} \int_{S_0} \nabla \times \frac{\dot{\mathbf{J}}(\mathbf{r}', \tau)}{R} dS' \quad (8)$$

where S_0 denotes the surface with the contribution due to the singularity at $\mathbf{r} = \mathbf{r}'$ or $R = 0$, removed from the surface S . Now, by substituting (8) into (2), we obtain

$$\frac{\dot{\mathbf{J}}(\mathbf{r}, t)}{2} - \mathbf{n} \times \frac{1}{4\pi} \int_{S_0} \nabla \times \frac{\dot{\mathbf{J}}(\mathbf{r}', \tau)}{R} dS' = \mathbf{n} \times \dot{\mathbf{H}}^i(\mathbf{r}, t). \quad (9)$$

By combining (1) and (9), the time-domain combined field equation (TD-CFIE) can be obtained.

$$\begin{aligned} \kappa \left[-\dot{\mathbf{E}}^s(\mathbf{r}, t) \right]_{\tan} + (1 - \kappa) \eta_0 \left[\frac{\dot{\mathbf{J}}(\mathbf{r}, t)}{2} - \mathbf{n} \times \frac{1}{4\pi} \int_{S_0} \nabla \times \frac{\dot{\mathbf{J}}(\mathbf{r}', \tau)}{R} dS' \right] \\ = \kappa \left[\dot{\mathbf{E}}^i(\mathbf{r}, t) \right]_{\tan} + (1 - \kappa) \eta_0 \mathbf{n} \times \dot{\mathbf{H}}^i(\mathbf{r}, t) \end{aligned} \quad (10)$$

where κ is the parameter of the linear combination, which is between 0 and 1, and η_0 is the wave impedance of free space. Using (3), (5), and (6), (10) can be written as

$$\begin{aligned} \kappa \left[\frac{1}{c} \int_S \frac{\ddot{\mathbf{J}}(\mathbf{r}', \tau)}{R} dS - c \nabla \int_S \frac{\nabla' \cdot \mathbf{J}(\mathbf{r}, \tau)}{R} dS \right]_{\tan} \\ + (1 - \kappa) \left[2\pi \dot{\mathbf{J}}(\mathbf{r}, t) - \mathbf{n} \times \nabla \times \int_S \frac{\dot{\mathbf{J}}(\mathbf{r}', \tau)}{R} dS \right] \\ = 4\pi \left[\frac{\kappa \dot{\mathbf{E}}_{\tan}^i(\mathbf{r}, t)}{\eta_0} + (1 - \kappa) \mathbf{n} \times \dot{\mathbf{H}}^i(\mathbf{r}, t) \right]. \end{aligned} \quad (11)$$

To solve Equation (11) numerically, the surface current density \mathbf{J} can be discretized in space and time. It is assumed that the total number of spatial and temporal basis functions are N_s and N_t , respectively. Then the current can be approximated as

$$\mathbf{J}(\mathbf{r}, t) = \sum_{j=1}^{N_t} \sum_{n=1}^{N_s} J_{j,n} T_j(t) \mathbf{f}_n(\mathbf{r}) \quad (12)$$

where the $J_{j,n}$ are the unknown coefficients. \mathbf{f}_n is the vector spatial basis function. Usually, the RWG basis function [26] is used for them. $T_j(t)$ is the scalar temporal basis function. Doing temporal and spatial testing with function $\Gamma_i(t)$ and $\mathbf{f}_m(\mathbf{r})$, and considering

$$\nabla \times \frac{\mathbf{J}(\mathbf{r}', \tau)}{R} = \frac{1}{c} \dot{\mathbf{J}}(\mathbf{r}', \tau) \times \frac{\hat{\mathbf{R}}}{R} + \mathbf{J}(\mathbf{r}', \tau) \times \frac{\hat{\mathbf{R}}}{R^2} \quad (13)$$

where $\hat{\mathbf{R}}$ is a unit vector along the direction $\mathbf{r} - \mathbf{r}'$, we have

$$\sum_{n=1}^{N_s} \left[\kappa Z_{mn}^E + (1 - \kappa) Z_{mn}^H \right] = V_{i,m} \quad (14)$$

$$Z_{mn}^E = A_{mn} - B_{mn} \quad (15)$$

$$Z_{mn}^H = 2\pi C_{mn} - D_{mn} \quad (16)$$

$$A_{mn} = \frac{1}{c} \int_S \mathbf{f}_m(\mathbf{r}) \cdot \int_S \frac{\mathbf{f}_n(\mathbf{r}') \int_0^\infty \Gamma_i(t) \sum_{j=1}^{N_t} J_{j,n} \ddot{T}_j(\tau) dt}{R} dS' dS \quad (17)$$

$$B_{mn} = c \int_S \nabla \cdot \mathbf{f}_m(\mathbf{r}) \int_S \frac{\nabla' \cdot \mathbf{f}_n(\mathbf{r}') \int_0^\infty \Gamma_i(t) \sum_{j=1}^{N_t} J_{j,n} T_j(\tau) dt}{R} dS' dS \quad (18)$$

$$C_{mn} = \int_S \mathbf{f}_m(\mathbf{r}) \cdot \mathbf{f}_n(\mathbf{r}) \int_0^\infty \Gamma_i(t) \sum_{j=1}^{N_t} J_{j,n} T_j(t) dt dS \quad (19)$$

$$D_{mn} = \int_S \mathbf{f}_m(\mathbf{r}) \cdot \mathbf{n} \times \int_S \mathbf{f}_n(\mathbf{r}') \times \hat{\mathbf{R}} \left[\frac{\int_0^\infty \Gamma_i(t) \sum_{j=1}^{N_t} J_{j,n} \ddot{T}_j(\tau) dt}{cR} + \frac{\int_0^\infty \Gamma_i(t) \sum_{j=1}^{N_t} J_{j,n} \dot{T}_j(\tau) dt}{R^2} \right] dS' dS \quad (20)$$

$$V_{i,m} = 4\pi \int_S \mathbf{f}_m(\mathbf{r}) \cdot \int_0^\infty \Gamma_i(t) \left[\frac{\kappa \dot{\mathbf{E}}^i(\mathbf{r}, t)}{\eta_0} + (1 - \kappa) \mathbf{n} \times \dot{\mathbf{H}}^i(\mathbf{r}, t) \right] dt dS \quad (21)$$

where $m = 1, 2, \dots, N_s, i = 1, 2, \dots, N_t$. Equation (14) is the general combined field integral equation. In the original MOT method, we choose a piecewise linear function as temporal basis function. In the MOD method, the weighted Laguerre function is used as temporal basis function. Brief descriptions are introduced in the next two sections.

2.2. MOT Algorithm

The temporal basis function in the MOT algorithm can be represented in terms of a set of triangle functions

$$T_j(t) = \begin{cases} 1 - \frac{|t - j\Delta t|}{\Delta t}, & \text{for } -\Delta t \leq t - j\Delta t \leq \Delta t \\ 0, & \text{otherwise} \end{cases} \quad (22)$$

where $j = 1, 2, \dots, N_t$ and Δt is time step. The point matching method can be used for temporal testing and the temporal testing function is

$$\Gamma_i = \delta(t - i\Delta t). \quad (23)$$

Then the temporal integral term in (17) can be calculated

$$\int_0^\infty \Gamma_i(t) \sum_{j=1}^{N_t} J_{j,n} \ddot{T}_j(\tau) dt = \sum_{j=1}^i J_{j,n} \ddot{T}_j \left(i\Delta t - \frac{R}{c} \right). \quad (24)$$

Similar results can be obtained for (18)–(21). Because the temporal basis function does not have continuous derivative, the derivative of the current is approximated by a finite difference [1–4]. Some researchers have used other temporal basis function that has successive continuous derivatives [6, 7].

In Equation (14) at time step i , the unknown coefficients $J_{i,n}$ can be solved by assuming that the currents up to the $i - 1$ step are known. Because it is a causal problem the currents at all time step of interest can be computed recursively.

2.3. MOD Algorithm

In the MOD algorithm, instead of a piecewise function, an entire domain function is used as temporal basis function and N_t can be set to ∞ . Therefore

$$T_j(t) = e^{-st/2} L_j(st) \quad (25)$$

where $L_j(t)$ is the Laguerre function of degree j and s is the scaling factor. The temporal testing function is also chosen weighted with the Laguerre function. Because of the orthogonality of the weighted Laguerre function, the first and second derivative of the basis functions can be written analytically as [20]

$$\sum_{j=0}^{\infty} J_{j,n} \dot{T}_j(st) = s \sum_{j=0}^{\infty} \left[\frac{1}{2} J_{j,n} + \sum_{k=0}^{j-1} J_{k,n} \right] T_j(st) \quad (26)$$

$$\sum_{j=0}^{\infty} J_{j,n} \ddot{T}_j(st) = s^2 \sum_{j=0}^{\infty} \left[\frac{1}{4} J_{j,n} + \sum_{k=0}^{j-1} (j-k) J_{k,n} \right] T_j(st) \quad (27)$$

with the assumption that $T_j(0) = 0$ and $\dot{T}_j(0) = 0$. These assumptions are valid since the transient waveforms are causal. Then Equation (14) can be solved using a MOD procedure. Details of the algorithm can be obtained in [20].

3. NUMERICAL RESULTS

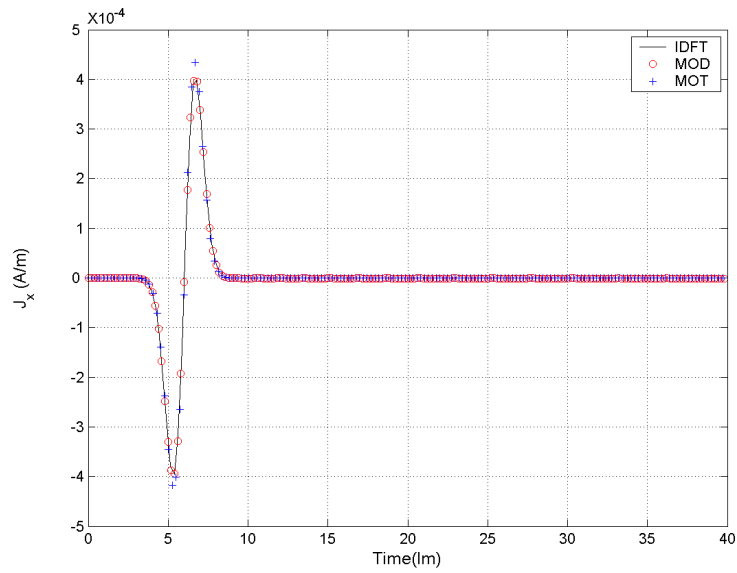
3.1. Stability

The first example considered is the scattering from a simple plate with size of $0.3 \text{ m} \times 0.3 \text{ m}$. Because the structure is open, only TD-EFIE can be applied. Here we use a pulse with a Gaussian shape as the incident wave. The Gaussian pulse can be mathematically represented by

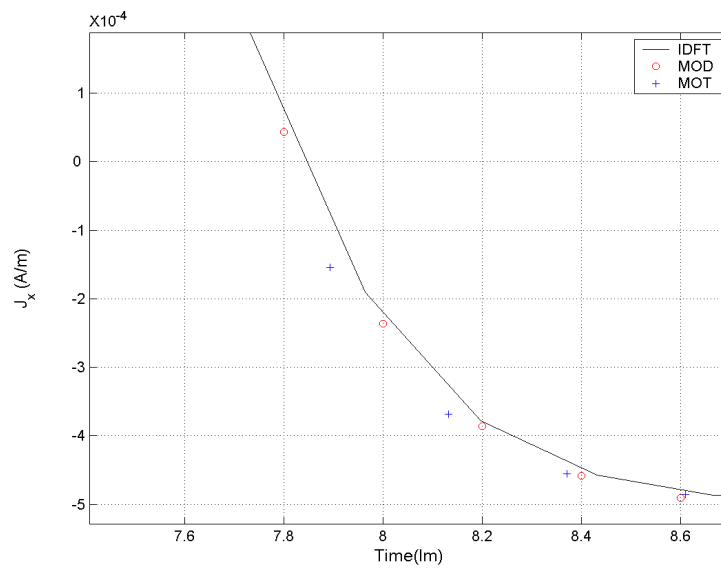
$$\mathbf{E}(\mathbf{r}, t) = \mathbf{E}_0 \frac{4}{T\sqrt{\pi}} e^{-\gamma^2} \quad (28)$$

where $\gamma = (4/T)(ct - ct_0 - \mathbf{r} \cdot \mathbf{k})$. T is the width of the pulse and ct_0 is the time delay at which the pulse reaches its peak. Both of these quantities are defined in light meters (lm). In our test examples, $T = 4 \text{ lm}$ and $ct_0 = 6 \text{ lm}$. \mathbf{k} is the wave vector for the incident wave. Fig. 1(a) shows the induced current at the center of the plate by the MOT and MOD methods with the inverse discrete Fourier transform (IDFT) of the frequency-domain result. In order to see the difference clearly, Fig. 1(b) shows the enlarged part of it. We compare the stability for different mesh size and different number of temporal basis functions both for the MOT and MOD method in Table 1. In Table 1, R_{\min} is the minimum distance between two nodes of the structure. The results of the MOD method are always stable if N_s is larger than a certain number which depends on the bandwidth of the incident signal and duration of the calculation [19].

For the MOT method, the results are often unstable for the explicit case. For the implicit case, it appears to be stable when a careful choice of the time step is made. It seems in this case the proper time step is around $0.2 \sim 0.3 \text{ lm}$. When the solution is unstable, the errors are amplified at each time step. The growth of the error is governed by the number of time steps and not by the total time and quickly becomes large enough to swamp the solution. The instability can often be reduced or eliminated for a particular mesh by averaging the current in time [5, 12] or space [10, 13]. These schemes typically



(a)



(b)

Figure 1. Induced current at the center of the plate. (a) Whole duration, (b) zoom out part of (a).

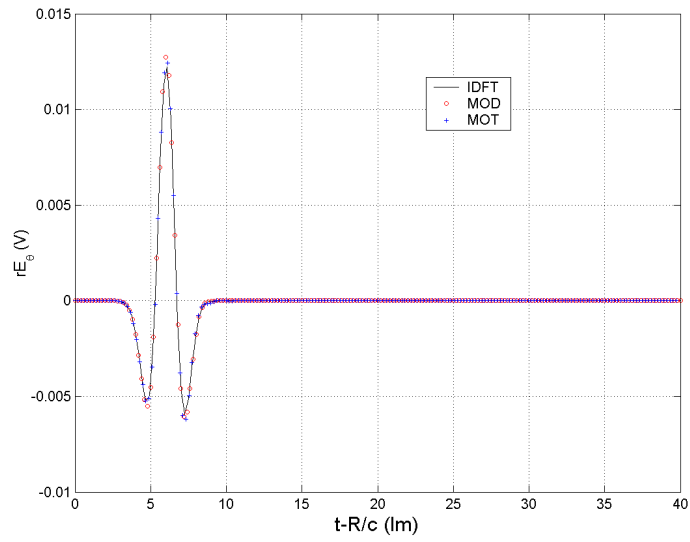
Table 1. Comparison of the results for the scattering from a plate.

N_s	MOD		MOT				
	N_t	CPU time (s)	$c\Delta t/R_{\min}$	$c\Delta t$ (lm)	N_t	Instability occurs beyond (steps)	CPU time (s)
79	73	41	0.5	0.013	3,072	80	
	120	113	4	0.10	384	270	
	150	201	8	0.21	192	Stable	4
	180	282	12	0.31	128	Stable	2.6
183	73	143	0.5	0.001	4,214	70	
	120	403	4	0.076	526	210	
	150	667	8	0.15	263	220	
	180	982	12	0.23	175	Stable	18
251	73	373	0.5	0.0075	5,351	90	
	120	1,089	8	0.12	334	230	
	150	1,815	12	0.18	222	170	
	180	2,793	16	0.24	167	Stable	47

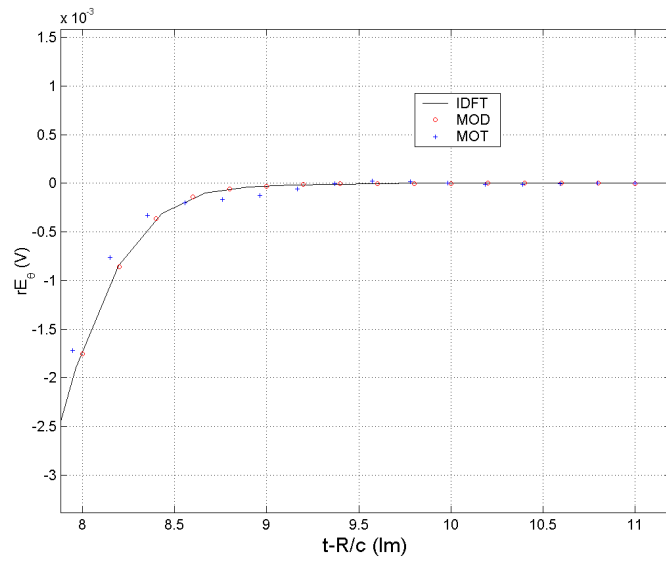
become unstable as more mesh points are used or more time steps are calculated. This means even if a method appears to be stable for one particular mesh and up to a specific time duration it cannot be assumed that it will be stable for another finer mesh or if the computations are made for a longer time duration. But for the MOD method, because the basis function is of entire domain and it decays to zero, MOD will never blow up in late time calculating duration.

3.2. Cost

Normally, the cost for the MOT and MOD methods are $O(N_t N_s^2)$ and $O(N_t^2 N_s^2)$, respectively. However, N_t for the MOT and MOD are not the same. N_t for the MOD method represents the time-bandwidth product of the waveforms to be approximated whereas N_t for the MOT method represents the number of time steps. In general, the cost of MOD is thus much larger than MOT when the number of time steps is not too large. Some technique such as interpolation can be used to speed up the MOT method. The computation time also depends on the method for the integral calculation. If we use a central approximation,



(a)



(b)

Figure 2. Backward scattered field from the sphere. (a) Whole duration, (b) zoom out part of (a).

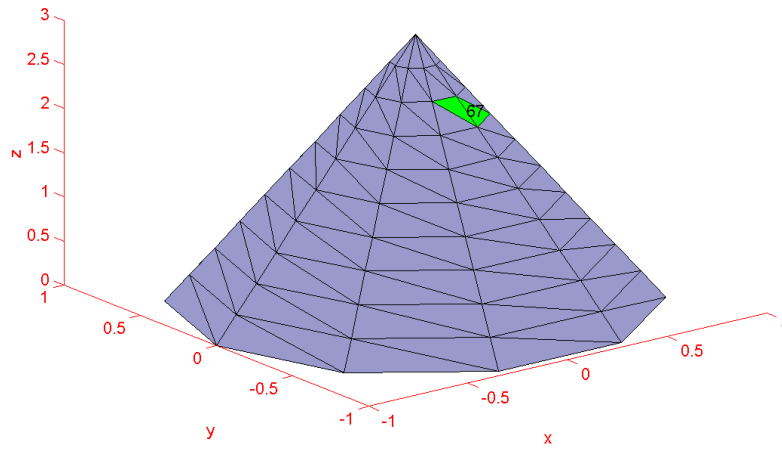


Figure 3. A conducting cone.

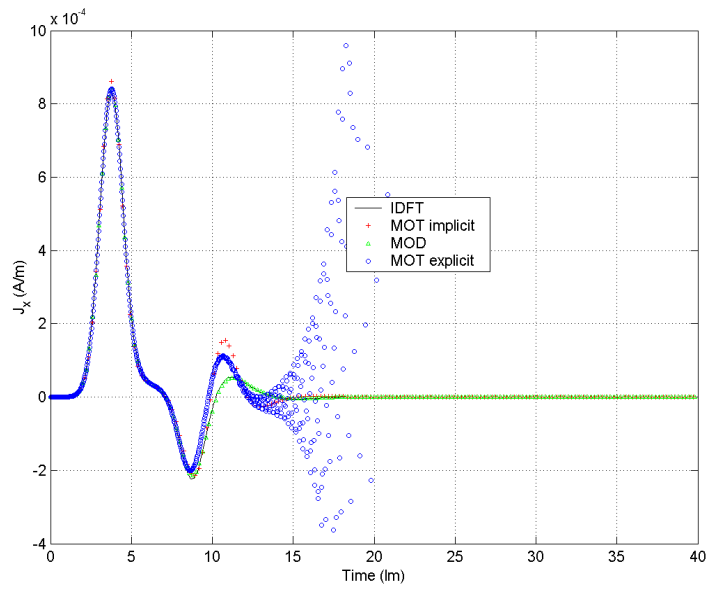


Figure 4. The induced current across edge 67 of the cone.

Table 2. Comparison of the results of a sphere.

N_s	MOD		MOT		FD-CFIE	
	Memory (MB)	CPU time (s)	Memory (MB)	CPU time (s)	Memory (MB)	CPU time (s)
540	93	2,022	89	242	23	5,546
1836	4,041	29,722	594	2,778	86	49,920

the integrals only need to be calculated once. We use another example to compare the cost for each of the methods. The scattering from a sphere with a radius of 0.2m and with different discretization is computed. Because it is a closed structure, we can use TD-CFIE ($\kappa = 0.5$). Table 2 shows the comparison of the results. For the MOT method ($c\Delta t = 0.2\text{lm}$), the time step is carefully chosen to get a stable result. MOD ($N_t = 73$) method uses much more CPU time and memory than that of MOT method. We also compare the result with that of the frequency-domain CFIE (FD-CFIE) (128 frequency points). Fig. 2 shows the backward far field and compares it with the IDFT of the frequency-domain results.

3.3. Accuracy

To check the accuracy for these two methods another example is tested with a conducting cone as shown in Fig. 3. To ensure the accuracy of the integrals, an adaptive Gaussian integral algorithm is used. Fig. 4 shows the current across edge 67. We can see also the results for the implicit MOT which provides a stable result for this case, but it is not accurate as the MOD method when compared with the IDFT results. From Fig. 1(b) and Fig. 2(b), the same conclusion can be obtained. This is because the MOT method uses point matching method for temporal testing, but the MOD method uses a Galerkin's method. Another point is the derivative of the current can be obtained analytically in the MOD method instead of finite difference in the MOT method.

4. CONCLUSION

In this paper, a comparison between the MOT with MOD methods for a TDIE solver is presented through numerical examples. The MOD method is always unconditionally stable and more accurate than the

MOT method, but it may take more CPU time and memory. The MOT method may be stable for a specific time step and for a limited time duration. The conclusion of this comparison is that the MOD method can be used in any case and guarantee unconditionally stable solution.

ACKNOWLEDGMENT

This work was supported by the Korea Research Foundation Grant funded by the Korean Government (R05-2004-000-10063-0).

REFERENCES

1. Rao, S. M. and D. R. Wilton, "Transient scattering by conducting surfaces of arbitrary shape," *IEEE Trans. Antennas Propagat.*, Vol. 39, No. 1, 56–61, Jan. 1991.
2. Sarkar, T. K., W. Lee, and S. M. Rao, "Analysis of transient scattering from composite arbitrarily shaped complex structures," *IEEE Trans. Antennas Propagat.*, Vol. 48, No. 10, 1625–1634, Oct. 2000.
3. Jung, B. H. and T. K. Sarkar, "Time-domain electric-field integral equation with central finite difference," *Microwave Opt. Technol. Lett.*, Vol. 31, No. 6, 429–435, Dec. 2001.
4. Jung, B. H. and T. K. Sarkar, "Time-domain CFIE for the analysis of transient scattering from arbitrarily shaped 3D conducting objects," *Microwave Opt. Technol. Lett.*, Vol. 34, No. 4, 289–296, Aug. 2002.
5. Vechinski, D. A. and S. M. Rao, "A stable procedure to calculate the transient scattering by conducting surfaces of arbitrary shape," *IEEE Trans. Antennas Propagat.*, Vol. 40, No. 6, 661–665, June 1992.
6. Hu, J.-L., C. H. Chan, and Y. Xu, "A new temporal basis function for the time-domain integral equation method," *IEEE Microw. Wireless Compon. Lett.*, Vol. 11, No. 11, 465–466, Nov. 2001.
7. Weile, D. S., G. Pisharody, N. W. Chen, B. Shanker, and E. Michielssen, "A novel scheme for the solution of the time-domain integral equations of electromagnetics," *IEEE Trans. Antennas Propagat.*, Vol. 52, No. 1, 283–295, Jan. 2004.
8. Manara, G., A. Monorchio, and R. Reggiannini, "A space-time discretization criterion for a stable time-marching solution of the electric field integral equation," *IEEE Trans. Antennas and Propagat.*, Vol. 45, No. 3, 527–532, March 1997.

9. Davies, P. J., "Numerical stability and convergence of approximations of retarded potential integral equations," *SIAM J. Numer. Anal.*, Vol. 31, 856–875, June 1994.
10. Davies, P. J., "On the stability of time-marching schemes for the general surface electric-field integral equation," *IEEE Trans. Antennas Propagat.*, Vol. 44, No. 11, 1467–1473, Nov. 1996.
11. Shankar, B., A. A. Ergin, K. Aygün, and E. Michielssen, "Analysis of transient electromagnetic scattering from closed surfaces using a combined field integral equation," *IEEE Trans. Antennas Propagat.*, Vol. 48, No. 7, 1064–1074, July 2000.
12. Rynne, B. P. and P. D. Smith, "Stability of time marching algorithms for the electric field equation," *J. Electromagn. Waves Applicat.*, Vol. 4, 1181–1205, 1990.
13. Davies, P. J., "A stability analysis of a time marching scheme for the general surface electric field integral equation," *Appl. Nume. Math.*, Vol. 27, 33–57, 1998.
14. Tijhuis, A. G., "Toward a stable marching-on-in-time method for two-dimensional transient electromagnetic scattering problems," *Radio Sci.*, Vol. 19, 1311–1317, 1984.
15. Sadigh, A. and E. Arvas, "Treating the instabilities in marching-on-in-time method from a different perspective," *IEEE Trans. Antennas Propagat.*, Vol. 41, No. 12, 1695–1702, Dec. 1993.
16. Yla-Oijala, P., M. Taskiene, and J. Sarvas, "Surface integral equation method for general composite metallic and dielectric structures with junctions," *Progress In Electromagnetics Research*, PIER 52, 81–108, 2005.
17. Hanninen, I., M. Taskinen, and J. Sarvas, "Singularity subtraction integral formulae for surface integral equations with RWG, rooftop and hybrid basis functions," *Progress In Electromagnetics Research*, PIER 63, 243–278, 2006.
18. Wang, S., X. Guan, D. Wang, X. Ma, and Y. Su, "Electromagnetic scattering by mixed conducting/dielectric objects using higher-order MoM," *Progress In Electromagnetics Research*, PIER 66, 51–63, 2006.
19. Chung, Y.-S., T. K. Sarkar, and B. H. Jung, "Solution of a time-domain magnetic-field integral equation for arbitrarily closed conducting bodies using an unconditionally stable methodology," *Microwave Opt. Technol. Lett.*, Vol. 35, No. 6, 493–499, Dec. 2002.
20. Jung, B. H., Y.-S. Chung, and T. K. Sarkar, "Time-domain EFIE, MFIE, and CFIE formulations using Laguerre polynomials as temporal basis functions for the analysis of transient scattering

- from arbitrary shaped conducting structures,” *Progress In Electromagnetics Research*, PIER 39, 1–45, 2003.
21. Jung, B. H., T. K. Sarkar, Y.-S. Chung, M. Salazar-Palma, and Z. Ji, “Time-domain combined field integral equation using Laguerre polynomials as temporal basis functions,” *Int. J. Nume. Model.*, Vol. 17, No. 3, 251–268, 2004.
 22. Jung, B. H., T. K. Sarkar, and M. Salazar-Palma, “Time domain EFIE and MFIE formulations for analysis of transient electromagnetic scattering from 3-D dielectric objects,” *Progress In Electromagnetics Research*, PIER 39, 113–142, 2004.
 23. Jung, B. H., T. K. Sarkar, and Y.-S. Chung, “Solution of time domain PMCHW formulation for transient electromagnetic scattering from arbitrarily shaped 3-D dielectric objects,” *Progress In Electromagnetics Research*, PIER 45, 291–312, 2004.
 24. Poularikas, A. D., *The Transforms and Applications Handbook*, IEEE Press, 1996.
 25. Gradshteyn, I. S. and I. M. Ryzhik, *Table of Integrals, Series, and Products*, Academic Press, New York, 1980.
 26. Rao, S. M., D. R. Wilton, and A. W. Glisson, “Electromagnetic scattering by surfaces of arbitrary shape,” *IEEE Trans. Antennas Propagat.*, Vol. 30, No. 3, 409–418, May 1982.